Photoinduced Electron Transfer in Supramolecular Assemblies Composed of One-Shell and Two-Shell Dialkoxybenzene-Tethered Ru(II)−Tris(bipyridine) Derivatives and a Bipyridinium Cyclophane

Elke David,[1] Roland Born,[1] Evgeny Kaganer,[2] Ernesto Joselevich,[2] Heinz Dürr,[1] and Itamar Willner*,[2]

Contribution from Organische Chemie, Universität des Saarlandes, Fachbereich 11.2, 66041 Saarbrücken, Germany, and The Institute of Chemistry and The Farkas Center for Light-Induced Processes, The Hebrew University of Jerusalem, Jerusalem 91904, Israel

Received January 31, 1997[⊗]

Abstract: Photoinduced electron transfer reactions are characterized in supramolecular assemblies consisting of a series of Ru(II)−bipyridine complexes that include tethered dialkoxybenzene units **2**−**5** and cyclo[bis(*N*,*N*′-*p*-xylylene-4,4′-bipyridinium)], BXV^{4+} (**1**). Formation of supramolecular complexes between BXV^{4+} and the dialkoxybenzene π-donor sites, linked to the photosensitizers, yields effective electron transfer quenching in the non-covalent-bound dyads and polyads. Steady-state luminescence quenching experiments and time-resolved studies reveal that for the one-shell photosensitizers **3** and **5** that include six and two dialkoxybenzene units, respectively, supramolecular photosensitizer-BXV^{4+} assemblies of maximal stoichiometries corresponding to six and two, respectively, coexist with lower supramolecular stoichiometries and free photosensitizers in the systems. For the two-shell dialkoxybenzene-tethered photosensitizers **2** and **4** that include 12 and 4 π-donor binding sites, respectively, supramolecular assemblies with BXV^{4+} of maximal stoichiometries corresponding to 6 and 2 are derived. The association constant of BXV^{4+} to the functionalized branch of the two-shell photosensitizer is ca. 10-fold higher than that of the one-shell photosensitizer. The higher affinity of the two-shell photosensitizers to form supramolecular complexes with BXV^{4+} is attributed to the cooperative participation of two dialkoxybenzene sites in the association of one BXV^{4+} unit. The higher association constants of BXV^{4+} to the two-shell photosensitizers **2** and **4**, yields improved electron transfer quenching as compared to the one-shell chromophores **3** and **5**. The photogenerated redox-products formed in the supramolecular assemblies Ru^{3+}−bipyridine and $BXV^{\bullet 3+}$, recombine within the non-covalent-bound structures without dissociation. The back electron transfer rate of the photogenerated redox products in the dyads and polyads is relatively slow due to their spatial separation by repulsive electrostatic interactions.

Introduction

Substantial efforts have been directed over the last decade toward mimicking the vectorial photoinduced electron transfer and charge separation in the photosynthetic reaction center.[3] One approach of modeling the photosynthetic reaction center includes the synthesis of covalently linked donor−acceptor dyads,[4] triads,[5,6] and pentads.[7] The electron transfer products in these systems are generally stabilized against recombination by their spatial separation in the molecular arrays. Further stabilization of the photogenerated redox products in molecular triads was accomplished by the incorporation of the molecular assemblies in heterogeneous matrices, such as zeolites[8] or layered phosphates.[9] Structural alignment and rigidification of the molecular arrays in these systems results in the stabilization of the redox products against back electron transfer. Similarly, the formation of donor−acceptor supramolecular complexes between a molecular photosensitizer−acceptor triad and an electron donor was reported to result in the steric rigidification of the triad, leading to vectorial photoinduced electron transfer.[10]

* To whom correspondence should be addressed. Phone: 972-2-6585272. Fax: 972-2-6527715.

⊗ Abstract published in *Advance ACS Abstracts,* August 1, 1997.

(1) Universität des Saarlandes.

(2) The Hebrew University of Jerusalem.

(3) (a) Deisenhofer, J.; Epp, O.; Miki, K.; Huber, R.; Michel, H. *J. Mol. Biol.* **1984**, *180*, 385. (b) Deisenhofer, J.; Epp, O.; Miki, K.; Huber, R.; Michel, H. *Nature* **1985**, *318*, 618. (c) Chang, C. H.; Tiede, D.; Tang, J.; Smith, U.; Norris, J.; Schiffer, M. *FEBS Lett.* **1986**, *205*, 82.

(4) (a) Connolly, J. S.; Bolton, J. R. In *Photoinduced Electron Transfer, Part D;* Fox, M. A., Chanon, M., Eds.; Elsevier: Amsterdam, Section 6.2. (b) Cooley, L. F.; Headford, C. E. L.; Elliott, C. M.; Kelley, D. F. *J. Am. Chem. Soc.* **1988**, *110*, 6673.

(5) (a) Gust, D.; Moore, T. A. *Top. Curr. Chem.* **1991**, *159*, 103. (b) Gust, D.; Moore, T. A. *Science* **1989**, *244*, 35. (c) Moore, T. A.; Gust, D.; Moore, A. L.; Bensasson, R. V.; Seta, P.; Bienvenue, E. In *Supramolecular Photochemistry*; Balzani, V., Ed.; D. Reidel: Boston, 1987; p 283. (d) Gust, D.; Moore, T. A. In *Supramolecular Photochemistry*; Balzani, V., Ed.; D. Reidel: Boston, 1987; p 267. (e) Wasielewski, M. R.; Gains, G. L., III; Wiederrecht, G. P.; Svec, W. A.; Niemczyk, M. P. *J. Am. Chem. Soc.* **1993**, *115*, 10442.

(6) (a) Sanders, G. M.; van Dijk, M.; van Veldhuizen, A.; van der Plas, M. J. *J. Chem. Soc., Chem. Commun.* **1986**, 1311. (b) Wasielewski, M. R.; Niemczyk, M. P.; Svec, W. A.; Pewitt, E. B. *J. Am. Chem. Soc.* **1985**, *107*, 5562. (c) Mecklenburg, S. L.; Peek, B. M.; Erickson, B. W.; Meyer, T. J. *J. Am. Chem. Soc.* **1987**, *109*, 3297. (d) Danielson, E.; Elliott, C. M.; Mesket, J. W.; Meyer, T. J. *J. Am. Chem. Soc.* **1987**, *109*, 2519. (e) Johnson, D. G.; Niemczyk, M. P.; Minsek, D. W.; Widerrecht, G. P.; Svec, W. A.; Gaines, G. L., III; Wasielewski, M. R. *J. Am. Chem. Soc.* **1993**, *115*, 5692.

(7) (a) Kurreck, H.; Huber, M. *Angew. Chem., Int. Ed. Engl.* **1995**, *34*, 849. (b) Gust, D.; Moore, T. A.; Moore, A. L.; Lee, S.-J.; Bittersmann, E.; Luttrull, D. K.; Rehms, A. A.; DeGraziano, J. M.; DeGraziano, J. M.; Ma, X. C.; Gao, F.; Belfored, R. E.; Trier, T. T. *Science* **1990**, *248*, 199.

(8) Yonemoto, E. H.; Kim, Y. I.; Schmehl, R. H.; Wallis, J. O.; Shoulders, B. A.; Richardson, B. R.; Haw, J. F.; Mallouk, T. E. *J. Am. Chem. Soc.* **1994**, *116*, 10557.

(9) (a) Vermuelen, L. A.; Thompson, M. E. *Nature* **1992**, *358*, 656. (b) Ungashe, S. B.; Wilson, W. L.; Katz, H. E.; Scheller, G. R.; Putrinski, T. M. *J. Am. Chem. Soc.* **1992**, *114*, 8717.

S0002-7863(97)00338-7 CCC: $14.00

A different approach of organizing photosensitizer−acceptor dyads involves the noncovalent assembly of photosensitizer−acceptor supramolecular complexes. Complementary H-bonds between functionalized photosensitizers and electron acceptors were reported to yield supramolecular photosensitizer−acceptor dyads.[11] Structural alignment of donor−acceptor dyads *via* the formation of supramolecular complexes with cyclodextrins was reported to enhance the photoinduced charge separation.[12] Recently, we reported a novel approach to organize photosensitizer−acceptor dyad and "polyad" assemblies *via* the application of octopus-like multireceptor photosensitizers that form supramolecular complexes with several electron acceptor units by π-donor−acceptor interactions.[13]

It is established that *N,N′*-dialkylbipyridinium salts form π-donor−acceptor complexes with different electron-rich aromatic compounds.[14,15] The supramolecular complexes between dialkoxybenzenes and the bipyridinium cyclophane cyclo[bis(*N,N′-p*-xylylene-4,4′-bipyridinium)], BXV^{4+} (**1**), have been

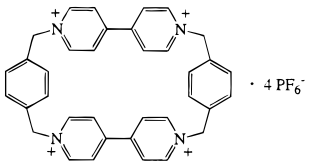

1

extensively studied by Stoddart and co-workers.[16,17] It was found that dialkoxybenzene intercalates into the bipyridinium cyclophane via π-donor-acceptor interactions, and the resulting supramolecular assemblies were applied in the synthesis of ingenious catenane macromolecules.[18,19]

In a previous paper we addressed the question of the photoinduced electron transfer in supramolecular assemblies formed between a series of multireceptor Ru(II)−polypyridine complexes and the bipyridinium cyclophane BXV^{4+} in an aqueous solution.[13] The photosensitizers consisted of a series of Ru(II)−tris(bipyridazine) complexes that included two, three, or six dialkoxybenzene groups tethered to the bipyridazine ligands of the chromophore through polyethylene glycol bridges. It was demonstrated that the dialkoxybenzene units provide receptor sites for the noncovalent association of the bipyridinium acceptor BXV^{4+}. The formation of the supramolecular complexes led to effective photoinduced electron transfer in the assemblies. It was further demonstrated that increasing the number of receptor sites on the chromophore enhances the photoinduced electron transfer. It was also shown that the noncovalently-linked supramolecular photosensitizer−electron acceptor polyads behave as intact entities where the photogenerated redox species recombine within the supramolecular assemblies. A detailed kinetic model that accounts for the electron transfer processes in these supramolecular polyads was formulated, and this enabled the quantitative analysis of the kinetics of photoinduced electron transfer and back electron transfer in the systems. In the reported series of chromophores, the maximum number of polyethylene glycol−dialkoxybenzene receptor sites tethered to the photosensitizer was six (two on each bidentate ligand). On the basis of the analyses of the photoinduced electron transfer in these supramolecular assemblies, it was suggested that the static photoinduced electron transfer processes in these supramolecular assemblies could be enhanced by designing multishell multireceptor arrays tethered to the central chromophore. That is, tethering a primary shell of dialkoxybenzene units, covalently-linked to a secondary shell of dialkoxybenzene sites, to the chromophore, would provide an effective molecular interface for the association of the electron acceptor units. Thereby, improved intramolecular photoinduced electron transfer is anticipated.

Here we report on the photoinduced electron transfer in supramolecular assemblies composed of one-shell and two-shell dialkoxybenzene multireceptor functionalized photosensitizers derived from Ru(II)−tris(bipyridine) **2**−**5** (Chart 1) and the electron acceptor BXV^{4+} (**1**). We examine the photoinduced electron transfer quenching pathways in the supramolecular assemblies and characterize the photogenerated redox products and their recombination in the one-shell and two-shell functionalized photosensitizers. We demonstrate that the two-shell modified photosensitizers do not show a simple additive effect in the association of the electron acceptor units of BXV^{4+}, but rather reveal a synergetic binding effect for the formation of the supramolecular complexes with the electron acceptor components. This synergetic association of BXV^{4+} to the two-shell functionalized photosensitizer is attributed to improved π-donor−acceptor interactions between BXV^{4+} and the two-shell receptor assembly, and it results in enhanced internal electron transfer within the resulting supramolecular systems.

Experimental Section

Absorption spectra were recorded with a Uvikon-860 (Kontron) spectrophotometer. Fluorescence spectra were recorded with a SFM-25 (Kontron) spectrofluorometer. Flash photolysis experiments were carried out with a Nd-YAG laser (Model GCR-150, Spectra Physics) coupled to a detection system (Applied Photophysics K-347) that included a monochromator and photomultiplier linked to a digitizer (Tektronix 2430 A) and computer for data storage and processing. This flash photolysis setup has a time resolution of >20 ns. For shorter time scale transients (>0.5 ns) a flash photolysis system consisting of

(10) Zahavy, E.; Seiler, M.; Marx-Tibbon, S.; Joselevich, E.; Willner, I.; Dürr, H.; O'Connor, D.; Harriman, A. *Angew. Chem., Int. Ed. Engl.* **1995**, *34*, 1005.

(11) (a) Sessler, J. L.; Wang, B.; Harriman, A. *J. Am. Chem. Soc.* **1993**, *115*, 10418. (b) Harriman, A.; Kubo, Y.; Sessler, J. L. *J. Am. Chem. Soc.* **1992**, *114*, 388. (c) Turró, C.; Chang, C. K.; Leroi, G. E.; Cukier, R. I.; Nocera, D. G. *J. Am. Chem. Soc.* **1992**, *114*, 4013. (d) Sun, L.; von Gersdorff, J.; Niethammer, D.; Tian, P.; Kurreck, H. *Angew. Chem., Int. Ed. Engl.* **1994**, *33*, 2318. (e) Sun, L.; von Gersdorff, J.; Sobek, J.; Kurreck, H. *Tetrahedron* **1995**, *21*, 471. (f) Dürr, H.; Bossmann, S.; Kropf, M.; Hayo, R.; Turro, N. J. *J. Photochem. Photobiol., A* **1994**, *80*, 341.

(12) Yonemura, H.; Nakamura, M.; Matsuo, T. *Chem. Phys. Lett.* **1989**, *155*, 157.

(13) Kropf, M.; Joselevich, E.; Dürr, H.; Willner, I. *J. Am. Chem. Soc.* **1996**, *118*, 655.

(14) (a) Willner, I.; Eichen, Y.; Rabinovitz, M.; Hoffman, R.; Cohen, S. *J. Am. Chem. Soc.* **1992**, *114*, 637. (b) Kisch, H.; Fernandez, A.; Wakatsuki, Y.; Yamazaki, H. *Z. Naturforsch.* **1985**, *406*, 292. (c) Nakamura, K.; Kai, Y.; Yasuoka, N.; Kasai, N. *Bull. Chem. Soc. Jpn.* **1981**, *54*, *3300*.

(15) (a) Usui, Y.; Misawa, H.; Sakuragi, H.; Tokumara, U. *Bull. Chem. Soc. Jpn.* **1987**, *60*, 1573. (b) Willner, I.; Eichen, Y.; Joselevich, E. *J. Phys. Chem.* **1990**, *94*, 3092.

(16) Anelli, P. L.; Ashton, P. R.; Ballardini, R.; Balzani, V.; Delgado, M.; Gandolfi, M. T.; Goodnow, T. T.; Kaifer, A. E.; Philip, D.; Pietraszkiewicz, M.; Prodi, L.; Reeddington, M. V.; Slavin, A. M. Z.; Spencer, N.; Stoddart, J. F.; Vincent, C.; Williams, D. J. *J. Am. Chem. Soc.* **1992**, *114*, 193.

(17) (a) Anelli, P. L.; Ashton, P. R.; Spencer, N.; Slawin, A. M. Z.; Stoddart, J. F.; Williams, D. J. *Angew. Chem., Int. Ed. Engl.* **1991**, *30*, 1036. (b) Ashton, P. R.; Odell, B.; Reddington, M. V.; Slawin, A. M. Z.; Stoddart, J. F.; Williams, D. J. *Angew. Chem., Int. Ed. Engl.* **1988**, *27*, 1550.

(18) (a) Anelli, P. L.; Spencer, N.; Stoddart, J. F. *J. Am. Chem. Soc.* **1991**, *113*, 5131. (b) Ashton, P. R.; Brown, C. L.; Chrystal, E. J. T.; Goodnow, T. T.; Kaifer, A. E.; Parry, K. P.; Slawin, A. M. Z.; Spencer, N.; Stoddart, J. F.; Williams, D. J. *Angew. Chem., Int. Ed. Engl.* **1991**, *30*, 1039. (c) Ashton, P. R.; Philip, D.; Spencer, N.; Stoddart, J. F. *J. Chem. Soc., Chem. Commun.* **1992**, 1124.

(19) (a) Bissell, R. A.; Cordova, E.; Kaifer, A. E.; Stoddart, J. F. *Nature* **1994**, *369*, 133. (b) Ashton, P. R.; Ballardini, R.; Balzani, V.; Gandolfi, M. T.; Marquis, D. J.-F.; Peréz-Garciá, L.; Prodi, L.; Stoddart, J. F.; Venturi, M. *J. Chem. Soc., Chem. Commun.* **1994**, 177. (c) Amabilino, D. B.; Ashton, P. R.; Reder, A. S.; Spencer, N.; Stoddart, J. F. *Angew. Chem., Int. Ed. Engl.* **1994**, *33*, 433.

Chart 1

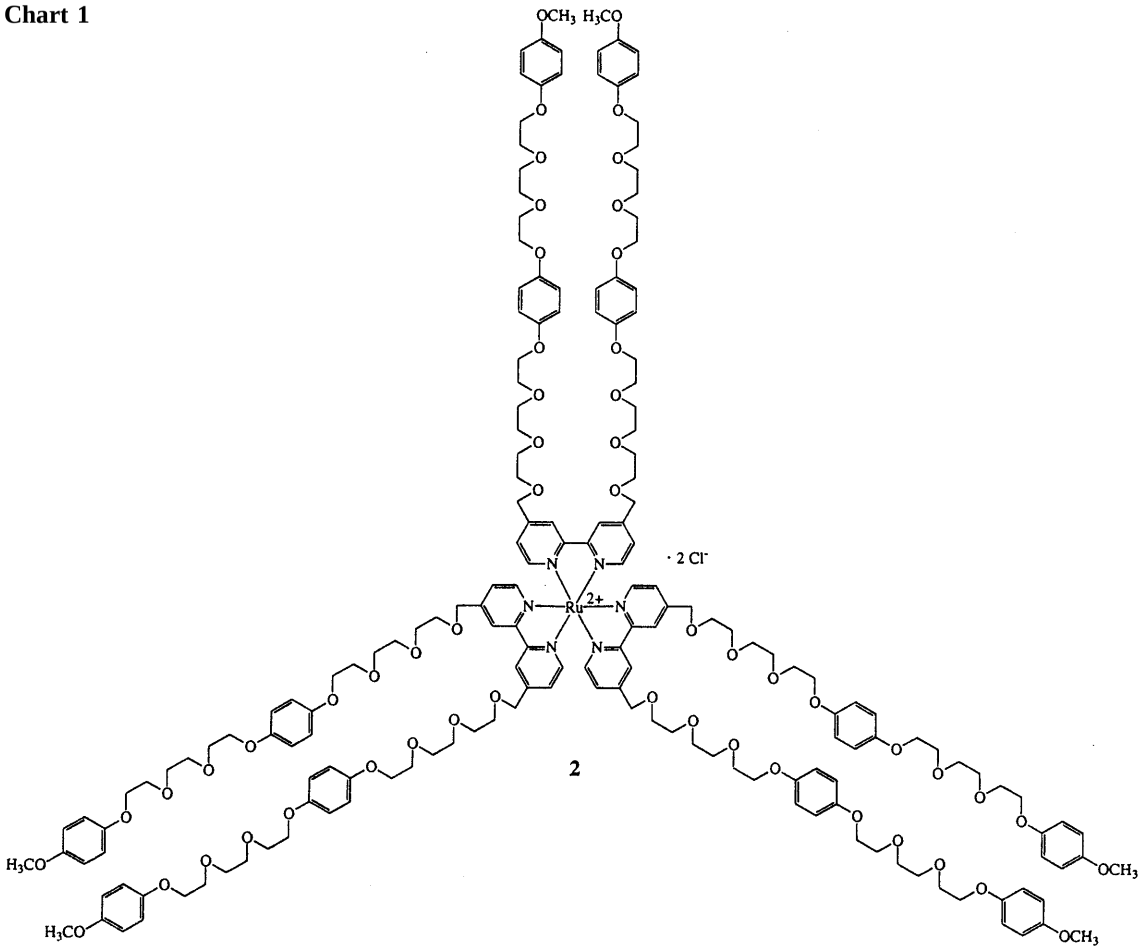
OCH3 H3CO
· 2 Cl-
Ru 2+
H3CO
OCH3

2

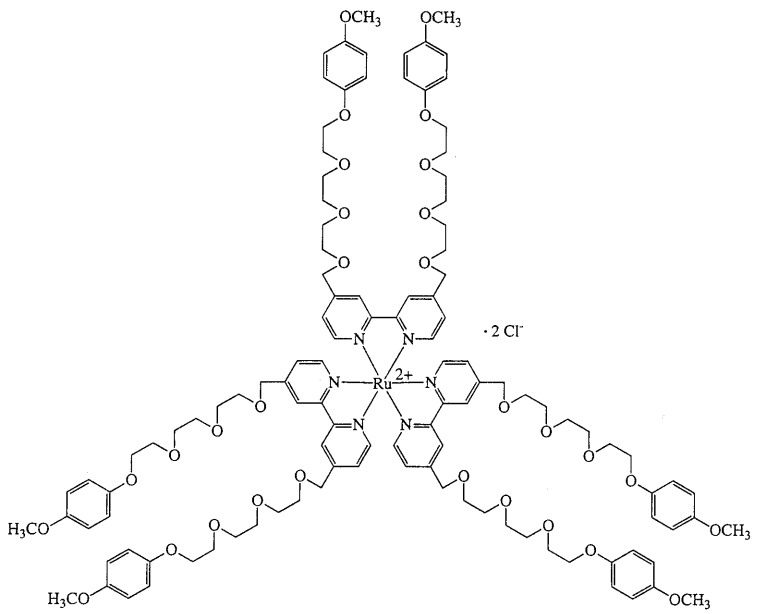
OCH3 OCH3
· 2 Cl-
Ru 2+
H3CO
OCH3

3

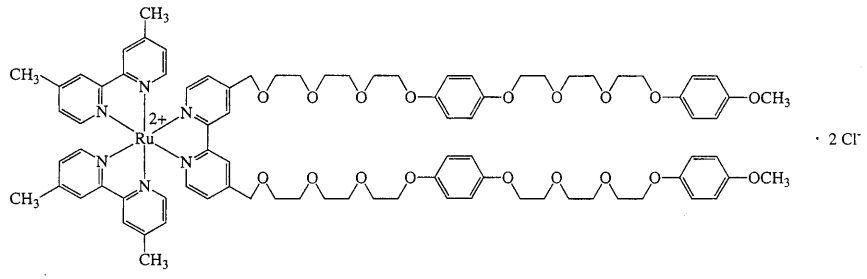
CH3
Ru 2+
OCH3
· 2 Cl-

4

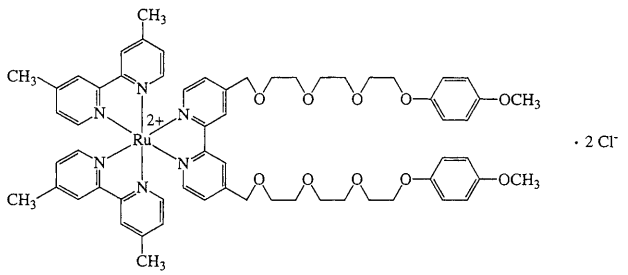
CH3
Ru 2+
OCH3
· 2 Cl-

5

a N_2 laser (PRA, LN-1000) coupled to a dye laser (Laser Photonics, Coumarin 460) was employed. These lasers were coupled to a detection system consisting of a monochromator and photomultiplier (Applied Photophysics) linked to a digitizer (Tektronix 7912 AD) and a computer for data storage and analysis.

All materials and solvents used in the synthesis of the ligands and the complexes were of highest purity from commercial sources (Aldrich). The acetonitrile which was used for the measurements was HPLC grade (JT Baker). Cyclo[bis(*N,N′-p*-xylylene-4,4′-bipyridinium)]-$(PF_6^-)_4m$ (**1**) was prepared according to the literature.[17b] The ligand 4,4′-bis[[[8-[[4-[(8-anisoxy-3,6-dioxaoct-1-yl)oxy]phenyl]oxy-3,6-dioxaoct-1-yl]ox]methyl]-2,2′-bipyridine was prepared by reacting 8-[[4-[(8-anisoxy-3,6-dioxaoct-1-yl)oxy]phenyl]oxy]-3,6-dioxa-1-octanol[20] (3.00 mmol) with 4,4′-bis(bromomethyl)-2,2′-bipyridine (1.50 mmol) in the presence of NaH (95%) (toluene, 12 h reflux), followed by chromatographic purification ($SiO_2/CH_2Cl_2-CH_3OH$ 95:5 (v/v) as eluent). The photosensitizer tris[4,4′-bis[[[8-[[4-[(8-anisoxy-3,6-dioxaoct-1-yl)oxy]-phenyl]oxy]-3,6-dioxaoct-1-yl]oxy]methyl]-2,2′-bipyridine]ruthenium-(II) dichloride (**2**) was prepared by the reaction of $Ru(DMSO)_4Cl_2$ (0.25 mmol) and the respective ligand (1.00 mmol) ($C_2H_5OH-H_2O$, 3:1 (v/v), 72 h reflux) followed by chromatographic purification ($SiO_2/CH_2Cl_2-CH_3OH$, 90:10 (v/v) as eluent). The photosensitizer bis(4,4′-dimethyl-2,2′-bipyridine)[4,4′-bis[[[8-[[4-[8-anisoxy-3,6-dioxaoct-1-yl)oxy]phenyl]oxy]-3,6-dioxaoct-1-yl]oxy]ethyle]-2,2′-bipyridine]-ruthenium(II) dichloride (**4**) was prepared by the reaction of Ru(II)−bis(4,4′-dimethyl-2,2′-bipyridine) (0.40 mmol) and the respective ligand (0.55 mmol) ($C_2H_5OH-H_2O$, 3:1, 72 h reflux) followed by chromatographic purification (SiO_2/CH_2Cl_2-CH_3OH, 95:5 (v/v) as eluent). The photosensitizers **3**, **5**, and **7** were prepared as reported earlier.[21] The photosensitizer **6** was prepared by the same procedure as **2** (*vide supra*), but using 4,4′-dimethyl-2,2′-bipyridyl (Aldrich) as ligand. All compounds gave satisfactory elementary analysis and ^{1}H-NMR spectra.

All photochemical measurements were performed in acetonitrile (JT Baker, HPLC grade). All steady-state luminescence and time-resolved quenching experiments were performed in 1 × 1 cm glass cuvettes that contained a solution of the respective photosensitizer in acetonitrile, 4.5×10^{-5} M (OD ≈ 1.0) and the appropriate concentration of the BXV^{4+}. In steady-state experiments, $\lambda_{ex} = 460$ nm, and in the transient experiments using the Nd-YAG laser, $\lambda_{ex} = 532$ nm and for the N_2-dye laser $\lambda_{ex} = 460$ nm. The resulting emission was recorded at $\lambda_{em} = 600$ nm. The recombination processes were characterized in acetonitrile solutions of the respective photosensitizer, 4.5×10^{-5} M, and BXV^{4+}, 2.5×10^{-3} M. For these absorption measurements, a pulsed Xe arc lamp (ORC, 250 W) was used. In order to obtain accurate absorption measurements, the signal component due to luminescence emission at the same wavelength was properly subtracted. All samples were deaerated by bubbling Ar for 20 min. All time-resolved and steady-state experiments were performed at a controlled constant temperature of 25 ± 2 °C.

Results and Discussion

The electron transfer quenching and charge separation processes were examined in a series of systems that included one of the Ru(II)−tris(bipyridine) derivatives **2**−**5**, acting as photosensitizer, and the electron acceptor bis[*N,N′-p*-xylylene-4,4′-bipyridinium], BXV^{4+} (**1**). All of these Ru(II)−bipyridine complexes include different numbers and configurations of dialkoxybenzene receptor groups capable of forming π-donor−acceptor charge transfer complexes with BXV^{4+}. The photosensitizers **3** and **5** contain six and two branches, respectively, where each branch includes one dialkoxybenzene group at the end of a triethylene glycol bridge. These two complexes can be regarded as one-shell multireceptor photosensitizers for BXV^{4+}. The photosensitizers **2** and **4** contain six and two branches, respectively, where each branch includes two dialkoxybenzene groups. One group is linked to the chromophore through a triethylene glycol bridge, and the second dialkoxybenzene group is attached to the first one through a second triethylene glycol chain. The latter two complexes, which include a total number of 12 or 4 dialkoxybenzene sites at two different distances from the metal center, can be regarded as two-shell multireceptor photosensitizers for BXV^{4+}.

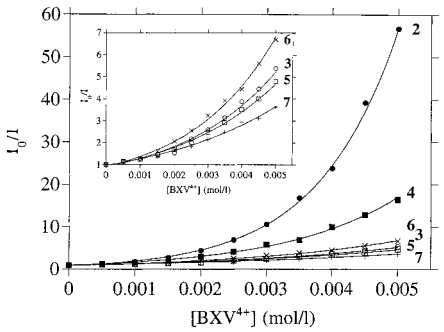

Figure 1. Stern−Volmer plots for the steady-state luminescence quenching of **2**−**7** by BXV^{4+}. All the photosensitizers are at a concentration of 4.5×10^{-5} M. Inset: Vertical zoom of the same plots for **3, 5, 6**, and **7**.

Steady-State Emission Experiments. Figure 1 shows the steady-state luminescence quenching of the series of complexes **2**−**5** by BXV^{4+} (**1**). Nonlinear Stern−Volmer plots are obtained for all of these photosensitizers, and the highest deviation from linearity is observed for **2**. The nonlinear Stern−Volmer plots indicate that the electron transfer quenching of the chromophores **2**−**5** by BXV^{4+} proceeds *via* a complex route that could be assigned to static quenching of the photosensitizer by BXV^{4+} units associated with the dialkoxybenzene sites and diffusional quenching of the free photosensitizer by BXV^{4+} (*vide infra*). It should be noted that the emission spectra of **2**−**7** are identical (except in their intensities) upon addition of BXV^{4+} in the entire concentration range. As control experiments, the luminescence quenching process of the photosensitizers **6** and **7** (Chart 2) by BXV^{4+} was examined. The latter photosensitizers lack the dialkoxybenzene binding sites, and thus formation of supramolecular complexes with BXV^{4+} is excluded. Nearly linear Stern−Volmer plots are obtained for the luminescence quenching of **6** and **7** by BXV^{4+} (Figure 1). Thus, the electron transfer quenching of **6** and **7** is diffusionally controlled. The minute deviation from linearity for compounds **6** and **7** can be attributed to slight changes in the ionic strength of the media upon addition of BXV^{4+}. It should be noted that the I_0/I values for reference compound **6** are slightly higher than for compounds **3** and **5**. This is attributed to the relative sizes and diffusion coefficients of the different photosensitizers. For the relatively small photosensitizer **6**, diffusional quenching is enhanced, as reflected by the higher diffusional quenching rate constants (*vide infra*, and Table 1).

Time-Resolved Emission Experiments. Further insight into the electron transfer quenching of the Ru(II)−bipyridine complexes **2**−**5** by BXV^{4+} is attained by time-resolved laser flash photolysis experiments. Figure 2 displays the transients of the luminescence decay of **2**−**5**, respectively, in the presence of different concentrations of BXV^{4+}. The luminescence transients reveal two important features: (i) the initial luminescence intensity decreases as the concentration of BXV^{4+} increases, and (ii) the luminescence lifetime is shortened as the concentration of BXV^{4+} increases. These features appear to be general for all of the photosensitizers **2**−**5** upon addition of BXV^{4+}. The magnitude of the decrease in the initial luminescence intensities and the extent of the shortening of the lifetimes

(20) The detailed synthesis of the ligand and the complexes will be described elsewhere. Dürr, H.; David, E. Manuscript in preparation.

(21) Seiler, M.; Dürr, H.; Willner, I.; Joselevich, E.; Doron, A.; Stoddart, J. F. *J. Am. Chem. Soc.* **1992**, *114*, 4013.

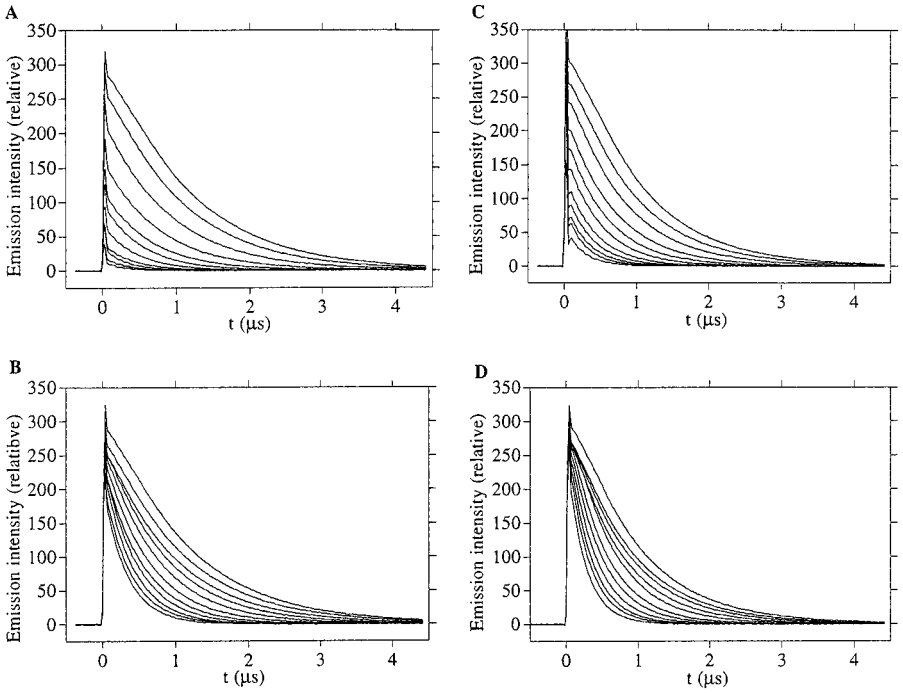

Figure 2. Transient luminescence intensities of (A) **2**, (B) **3**, (C) **4**, and (D) **5**, in the presence and absence of BXV^{4+}. Upper curves correspond to the photosensitizer luminescence without BXV^{4+}. All other transients represent the systems with added BXV^{4+} at consecutive increments of 5×10^{-4} M, up to an overall concentration of 5.0×10^{-3} M.

Chart 2

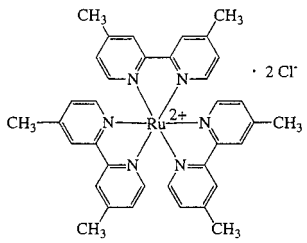

6

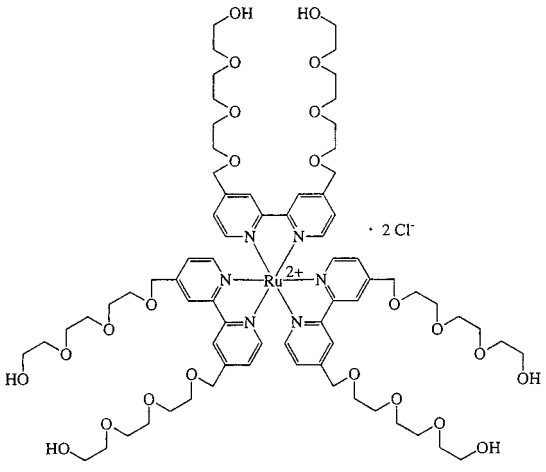

7

of the chromophores vary and depend on the structure of the photosensitizer.

Figure 3 shows the luminescence transients obtained upon addition of different concentrations of BXV^{4+} to the reference compounds **6** and **7**, respectively. In both cases we observe that the initial intensity remains nearly constant upon increasing the concentration of BXV^{4+}, but the luminescence lifetime is

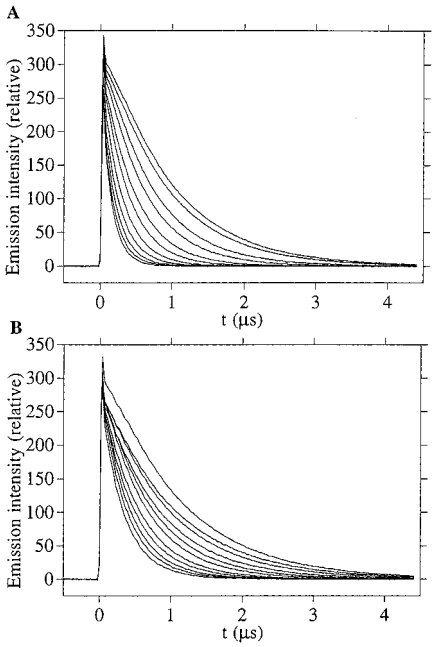

Figure 3. Transient luminescence intensities of the reference compounds (A) **6** and (B) **7** in the presence and absence of BXV^{4+}. Upper curves correspond to the photosensitizer luminescence without BXV^{4+}. All other transients represent the systems with added BXV^{4+} at consecutive increments of 5×10^{-4} M, up to an overall concentration of 5.0×10^{-3} M.

shortened. The latter behavior, where only the luminescence lifetime is shortened upon increasing the concentration of the electron acceptor, is characteristic of a diffusional electron transfer quenching. Thus, the unique features observed for the luminescence decay of the photosensitizers **2**−**5** by BXV^{4+}, consisting of a decrease in both initial luminescence intensity and luminescence lifetime, are attributed to the participation of two complementary electron transfer quenching pathways. Photosensitizers **2**−**5** include the dialkoxybenzene groups, and are capable of forming supramolecular complexes with the

bipyridinium cyclophane electron acceptor BXV^{4+}. Electron transfer quenching within the supramolecular assembly should proceed by a fast, nondiffusional, static pathway. Provided this fast quenching process occurs within a time scale shorter than the time resolution of the luminescence measurements, the static electron transfer quenching is reflected by a decrease in the measured "initial" luminescence intensity as actually observed. The resulting transient luminescence and the shortening of its lifetime are attributed to the free photosensitizer which is quenched by the electron acceptor BXV^{4+} via a diffusional route, similar to that occurring in the reference compounds **6** and **7**. The assignment of the decrease in the initial emission intensity to a fast static quenching process will be confirmed later by further experiments on a shorter time scale (*vide infra*). These transient luminescence features of the photosensitizers **2**−**5**, which include tethered dialkoxybenzene units, in the presence of BXV^{4+} are similar to the recently reported electron transfer quenching of alkoxyanisyl-tethered Ru(II)−tris(bipyridazine) complexes and BXV^{4+}.[13]

A qualitative comparison of the emission transients of the photosensitizers **2**−**5** in the presence of BXV^{4+}, Figure 2, allows clear differences between the one-shell and two-shell dialkoxybenzene-functionalized chromophores to be pointed out. The initial luminescence intensity, corresponding to the internal electron transfer quenching within the supramolecular assemblies, is substantially enhanced in the two-shell modified photosensitizers **2** and **4** as compared to the one-shell functionalized photosensitizers **3** and **5**, respectively. For example, at a concentration of BXV^{4+} corresponding to 5.0×10^{-3} M, the initial luminescence intensity of **2** decreases to 2%, whereas that of **3** decreases only to 19%. It is also evident that, for the two-shell photosensitizers **2** and **4**, increasing the number of dialkoxybenzene units enhances the quenching of the initial luminescence intensity. The qualitative analysis of the initial luminescence intensity quenching of the one-shell and two-shell photosensitizers reveals, however, that the effectiveness of the intramolecular quenching is not controlled only by the number of dialkoxybenzene units but also by their spatial configuration. For the two-shell photosensitizer **4**, a total number of four dialkoxybenzene units exists whereas in the one-shell photosensitizer **3**, six dialkoxybenzene units are present. The initial luminescence of **4** is, however, quenched more effectively than that observed for **3** (cf. parts B and C Figure 2). For example, for a BXV^{4+} concentration of 5.0×10^{-3} M, the initial luminescence intensity of **4** is decreased to 6%, whereas that of **3** (which includes six dialkoxybenzene sites) is quenched only to 19%. These results clearly imply that unique interactions in the two-shell photosensitizers lead to enhanced intramolecular electron transfer quenching in the resulting supramolecular assemblies.

Kinetic Model and Analysis of Electron Transfer in the Supramolecular Assemblies. To quantitatively analyze the electron-transfer quenching of photosensitizers **2**−**5** by the bipyridinium electron acceptor BXV^{4+}, and to determine the association constants of the resulting supramolecular assemblies, we apply the kinetic model that was previously developed by us[13] and corresponds to the electron transfer quenching of a multireceptor photosensitizer by an electron acceptor substrate. The kinetic model takes into consideration the photoprocesses of the multireceptor photosensitizer, S, in the presence of the electron acceptor, A, within the resulting supramolecular assemblies exhibiting all the possible stoichiometries: S, SA, SA_2, ..., SA_N (N is the number of binding sites on the photosensitizer), as well as the quenching of the photosensitizer by a diffusional route. The photosensitizer configurations are generally represented as SA_n ($n = 0, 1, 2, ..., N$), where the case $n = 0$ represents the unbound photosensitizer. The relevant processes, species and kinetic constants involved in the photoreactions of the different supramolecular photosensitizer states are summarized in eqs 1−9.

$$SA_{n-1} + A \underset{k_{-n}}{\overset{k_n}{\rightleftharpoons}} SA_n \quad (n = 1, 2, ..., N) \tag{1}$$

$$SA_n \xrightarrow{h\nu} S^*A_n \quad (n = 0, 1, 2, ..., N) \tag{2}$$

$$S^*A_{n-1} + A \underset{k^*_{-n}}{\overset{k^*_n}{\rightleftharpoons}} S^*A_n \quad (n = 1, 2, ..., N) \tag{3}$$

$$S^*A_n \xrightarrow{k_D} SA_n \quad (n = 0, 1, 2, ..., N) \tag{4}$$

$$S^*A_n + A \xrightarrow{k_{dq}} S^+A_n + A^- \quad (n = 0, 1, 2, ..., N) \tag{5}$$

$$S^*A_n \xrightarrow{k_{sq}} S^+A^-A_{n-1} \quad (n = 1, 2, ..., N) \tag{6}$$

$$S^+A_n + A^- \xrightarrow{k_{dr}} SA_n + A \quad (n = 0, 1, 2, ..., N) \tag{7}$$

$$S^+A^-A_{n-1} \xrightarrow{k_{sr}} SA_n \quad (n = 1, 2, ..., N) \tag{8}$$

$$S^+A^-A_{n-1} \xrightarrow{k_{esc}} S^+A_{n-1} + A^- \quad (n = 1, 2, ..., N) \tag{9}$$

These equations represent the following processes: (1) association and dissociation of the photosensitizer and electron acceptor in the ground state; (2) photoexcitation; (3) association and dissociation of the photosensitizer and acceptor in the excited state; (4) natural decay of the photosensitizer; (5) diffusional electron transfer quenching; (6) static electron transfer quenching within the supramolecular assemblies; (7) diffusional back electron transfer of the photogenerated redox products; (8) static back electron transfer recombination of the redox species within the supramolecular assemblies; (9) escape or dissociation of the redox products from the supramolecular assemblies.

The main assumptions adopted in the kinetic model, and the development of the consequent kinetic equations, were discussed and justified in our previous paper.[13] Two important assumptions of this model are that (i) the diffusional quenching rate is proportional to the electron acceptor concentration and (ii) the static quenching rate of the photosensitizer for each supramolecular assembly is proportional to the stoichiometry, i.e., to the number of electron acceptor units bound to the photosensitizer.

As a result of these assumptions, we find that different stoichiometries of supramolecular assemblies SA_n($n = 0, 1, 2, ..., N$) are found in equilibrium in the system prior to excitation, and their concentrations, which are characteristic of a standard binomial distribution, are given by eq 10, where S_o is the

$$[SA_n] = \frac{S_o}{(1 + K[A])^N} \frac{N!}{n!(N-n)!} K^n[A]^n \quad (n = 0, 1, 2, ..., N) \tag{10}$$

analytical concentration of the multireceptor photosensitizer, N is the maximal stoichiometry, i.e., the number of binding sites on the multireceptor photosensitizer, and K is the association constant between one binding site and the electron acceptor, A. Upon pulse photoexcitation of the system, equal fractions

of every population are promoted to the excited states S^*A_n, and immediately after excitation, their distribution is similar to the ground-state distribution. As each population decays at a different rate, the overall decay of the luminescence of the photosensitizer is multiexponential. The transient emission decay according to this model is given by eq 11, where $I(0)$ is

$$I(t) = I(0)e^{-(k_D+k_{dq}[A])t}\left(\frac{1+K[A]e^{-k_{sq}t}}{1+K[A]}\right)^N \qquad (11)$$

the emission intensity immediately after photoexcitation, k_{dq} is the rate constant of the diffusional quenching process for all the excited photosensitizer populations, and k_{sq} is the first-order kinetic rate constant of the static quenching per electron acceptor unit (the rate constant of the static quenching associated with each population SA_n is nk_{sq}).

Since the static quenching is much faster than the diffusional quenching ($k_{sq} >> k_{dq}[A]$), the transient luminescence is composed of a fast decay which is attributed to the static quenching in the supramolecular assemblies, SA_n ($n = 1, 2, ..., N$), and a slow decay which is attributed to natural decay and diffusional quenching of the unbound photosensitizer, S. The fast decay ends when the term $K[A]\exp(-k_{sq}t)$ in eq 11 becomes negligible, and then the slow emission, $I_{slow}(t)$, is expressed by eq 12.

$$I_{slow}(t) = I(0)\frac{1}{(1+K[A])^N}e^{-(k_D+k_{dq}[A])t} \qquad (12)$$

The emission transients shown in Figure 2 are assigned to the slow emission decay, $I_{slow}(t)$, of the free photosensitizer (eq 12). The apparent decrease in the initial luminescence as the concentration of the acceptor BXV^{4+} is increased is attributed to the fast static quenching (not seen on this time scale) of higher fractions of bound photosensitizer, and the accompanying shortening of the luminescence lifetime is interpreted as a result of the diffusional quenching of the free photosensitizer (the fast decay due to static quenching was confirmed in complementary experiments performed on shorter time scales, *vide infra*). The emission transients corresponding to the luminescence decay of the photosensitizers including dialkoxybenzene groups (**2**−**5**) with addition of BXV^{4+} (Figure 2) are hence characterized by this apparent decrease in the observed initial emission intensity, whereas the emission transients corresponding to the emission decay of the reference photosensitizers lacking the dialkoxybenzene groups (**6** and **7**), Figure 3, are only characterized by a shortening of the lifetime upon addition of BXV^{4+}, with almost no change in the observed initial emission intensity.

A quantitative interpretation of the Stern−Volmer plots shown in Figure 1 is possible by the formulated model. Assuming that the steady-state luminescence intensity of the photosensitizer at any concentration of electron acceptor is proportional to the integration over time of the transient luminescence intensity (eq 11), and realizing that the term $K[A]\exp(-k_{sq}t)$, related to the fast decay, quickly becomes null and does not contribute significantly to the integrated luminescence, the Stern−Volmer plots can be expressed by means of eq 13, where I_o and I are

$$\frac{I_o}{I} = (1+K[A])^N\frac{\tau_o}{\tau} \qquad (13)$$

the steady-state luminescence intensities in the absence and in the presence of variable concentrations of electron acceptor, respectively, and τ_o and τ are the luminescence lifetimes in the absence and in the presence of the electron acceptor, respectively. An expression for the luminescence lifetime can also be obtained from eq 11, as shown in eq 14.

$$1/\tau = k_D + k_{dq}[A] \qquad (14)$$

Equation 13 explains the nonlinearity of the Stern−Volmer plots shown in Figure 1, since, although the term τ_o/τ is linear, the term $(1 + K[A])^N$ is a polynomial of degree N. That is, the Stern−Volmer plots corresponding to the quenching of the multireceptor photosensitizers **2**−**5** can be described as polynomials of degree $N + 1$, where N is the number of binding sites. When K is null, as with the reference compounds **6** and **7**, the Stern−Volmer plots are linear.

Figure 4 shows the shortening of the lifetimes of the photosensitizers **2**−**5** upon addition of variable concentrations of BXV^{4+} by analysis of the transients shown in Figure 2. The diffusional electron transfer rate constants, k_{dq}, of the different free photosensitizers, were calculated from these plots using eq 14. The values are summarized in Table 1. We see that the diffusional electron transfer rates of the different photosensitizers are within the same range of values. The slight deviation, which is also detected in the reference compounds **6** and **7**, can be attributed to a change in the ionic strength of the media upon addition of BXV^{4+}.

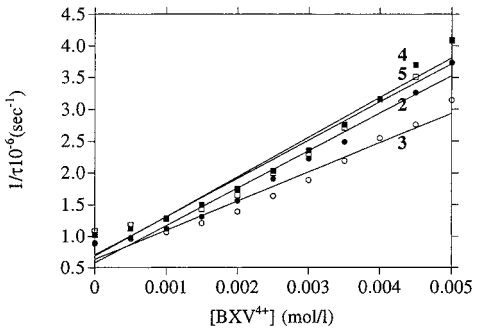

Figure 4. Shortening of the lifetime of the slow luminescence decay at different concentrations of BXV^{4+}. Data for lifetimes were extracted from Figure 2.

Table 1. Diffusional and Static Electron Transfer Quenching Rate Constants in the Photosensitizer−BXV^{4+} Systems and the Association Constants of the Resulting Supramolecular Assemblies

photosensitizer	$10^6\tau_o$ (s^{-1})	$10^{-9}k_{dq}$[a] ($M^{-1}\ s^{-1}$)	$10^{-6}k_{sq}$[b] (s^{-1})	K[c] (M^{-1})
2	1.14	0.59	170	110 ± 10 (90 ± 10)
3	1.12	0.46	150	10 ± 2 (15 ± 2)
4	0.98	0.63	220	210 ± 20 (190 ± 20)
5	0.92	0.60	200	20 ± 4 (50 ± 20)
6	1.00	1.20		
7	0.98	0.44		

[a] Deduced from the shortening of the slow-decay luminescence lifetimes. [b] Obtained by fitting the fast luminescence decay to eq 11. [c] Derived from the modified Stern−Volmer plots, according to eq 15. The association constants in parentheses correspond to the values obtained from the fitting of the fast luminescence decay to eq 11.

Analysis of Supramolecular Association and Stoichiometry. The association parameters and nature of supramolecular assemblies formed between the series of photosensitizers **2**−**5** and BXV^{4+} can be analyzed by means of a modified Stern−Volmer equation corresponding to the quenching of a multireceptor photosensitizer by a substrate quencher, which is obtained by rearrangement of eq 13 to the form of eq 15. This modified

$$\left(\frac{I_o}{I}\frac{\tau}{\tau_o}\right)^{1/N} = 1 + K[A] \qquad (15)$$

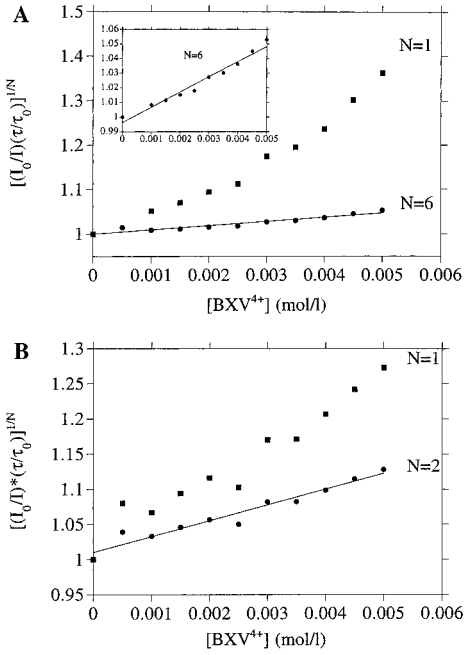

Figure 5. Modified Stern−Volmer plots for the luminescence quenching of (A) **3** and (B) **5** by BXV^{4+}, assuming different maximal supramolecular stoichiometries. Linear fitting is observed for **3** when $N = 6$ (see vertical zoom inset) and for **5** when $N = 2$.

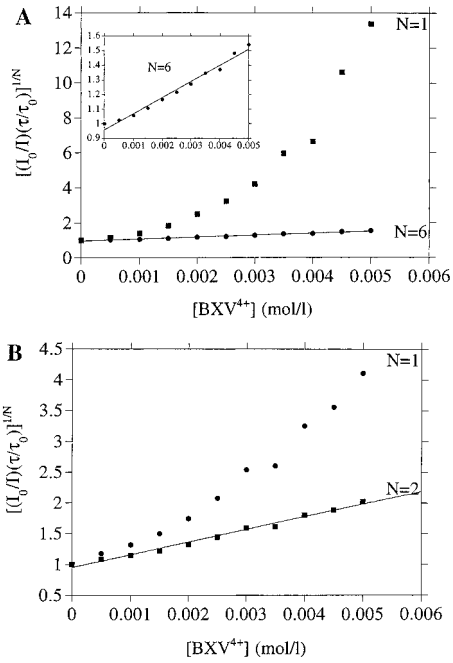

Figure 6. Modified Stern−Volmer plots for the luminescence quenching of (A) **2** and (B) **4** by BXV^{4+}, assuming different maximal supramolecular stoichiometries. Linear fitting is observed for **2** when $N = 6$ (see vertical zoom inset) and for **4** when $N = 2$.

Stern−Volmer equation contains the expression I_o/I of the standard Stern−Volmer plot, and the factor τ/τ_o which is obtained from time-resolved measurements. A linear modified Stern−Volmer plot, $[(I_o/I)(\tau/\tau_o)]^{1/N}$ vs the electron acceptor concentration, should be obtained upon selection of the appropriate maximal stoichiometry possible for the respective photosensitizer.

Figure 5 shows the modified Stern−Volmer plots for the one-shell photosensitizers **3** and **5**. For the photosensitizer **3**, which consists of six branches, each of which includes a single dialkoxybenzene unit, a linear relationship is obtained upon using $N = 6$ as the maximal stoichiometry of the supramolecular complex. All other values for possible stoichiometries do not lead to a linear relationship. From the linear plot for $N = 6$, Figure 5A, the derived association constant of BXV^{4+} to a dialkoxybenzene site corresponds to $K = 10 \pm 2\ M^{-1}$. The values of the association constants of BXV^{4+} to the binding site on a single chain are in good agreement with the reported association constant between BXV^{4+} and dimethoxybenzene in acetonitrile ($K_{ass} = 17\ M^{-1}$).[16] For photosensitizer **5**, Figure 5B, the linear Stern−Volmer plot is observed upon assuming the stoichiometry of the supramolecular complex, $N = 2$, consistent with the fact that the photosensitizer includes two chains with two dialkoxybenzene binding sites. The derived association constant corresponds to $K = 20 \pm 4\ M^{-1}$. Figure 6 shows the modified Stern−Volmer plot for the two-shell photosensitizers **2** and **4**. For the photosensitizer **2**, Figure 6A, which consists of six branches with two dialkoxybenzene sites in each branch, a linear modified Stern−Volmer plot is obtained upon assuming a maximal stoichiometry of $N = 6$. That is, although 12 binding sites are available for BXV^{4+}, the steady-state luminescence experiments imply the formation of a supramolecular complex of a maximal stoichiometry that corresponds to $N = 6$. From the slope of the linear plot shown in Figure 6A, the derived association constant of BXV^{4+} per branch is $K = 110 \pm 10\ M^{-1}$. Similar results are obtained upon analyzing the steady-state luminescence properties of **4** in the presence of BXV^{4+}. The latter two-shell complex consists of two branches that include two dialkoxybenzene units in each branch, and thus four binding sites for BXV^{4+} are available. The modified Stern−Volmer plot, Figure 6B, reveals, however, that a linear relationship is obtained upon assuming a maximal stoichiometry of $N = 2$. The derived association constant of BXV^{4+} per branch is $K = 210 \pm 20\ M^{-1}$.

Comparison of the BXV^{4+} association constants per branch for the one-shell and two-shell photosensitizers reveals substantial differences. The association constant of BXV^{4+} to a branch of the two-shell photosensitizers is ca. 10-fold higher than the association constant of BXV^{4+} to a branch of the one-shell photosensitizers. The higher affinities of the two-shell photosensitizers **2** and **4** for BXV^{4+} as compared with the analogous one-shell photosensitizers **3** and **5**, respectively, cannot be explained simply by the additive effect of an increase in the number of binding sites in the two-shell photosensitizers. If this was the case, then doubling the number of dialkoxybenzene groups on each chain tethered to the photosensitizer would lead to only a 2-fold increase in the association constant to BXV^{4+}. The 10-fold higher association constants to BXV^{4+} of the two-shell photosensitizers are thus attributed to a cooperative effect of the two dialkoxybenzene units available in each branch in the association of BXV^{4+}. The flexibility of the triethylene glycol chains linking the two dialkoxybenzene units would allow the intrachain formation of a π-stacked supramolecular complex that includes a bipyridinium/dialkoxybenzene/bipyridinium/dialkoxybenzene assembly, Figure 7. That is, one bipyridinium unit is sandwiched between two dialkoxybenzene sites available in each branch.

Several previous examples emphasize the π-stacking effect on the association constant of the resulting supramolecular assemblies. For example, the association of *N*,*N*′-dimethyl-4,4′-bipyridinium to a bis[dialkoxybenzene] cyclophane is higher than to dimethoxybenzene.[22] The π-stacking of BXV^{4+} to bis-[dialkoxybenzene] derivatives was also used in the successful synthesis of catenanes.[18,19] The stabilization of supramolecular complexes between BXV^{4+} and the two-shell photosensitizers via a π-stacking route explains the derived maximal stoichi-

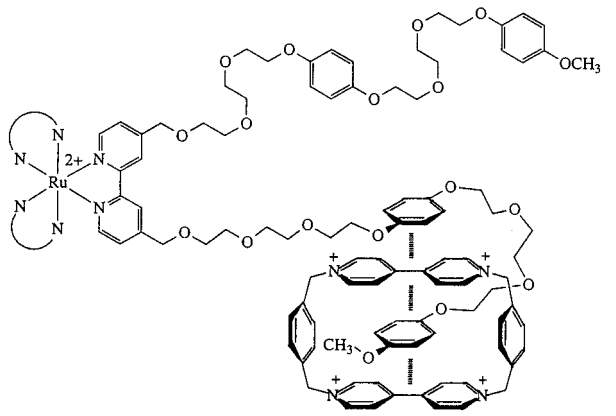

Figure 7. Schematic structure for the cooperative binding of BXV^{4+} by two adjacent dialkoxybenzene units of one branch of the two-shell multireceptor photosensitizers. The upper branch is free, and the lower one binds a BXV^{4+} unit.

ometries derived from the modified Stern−Volmer plots. Provided the two dialkoxybenzene units participate in the association of a single BXV^{4+}, the expected maximal stoichiometries for photosensitizers **2** and **4** are $N = 6$ and $N = 2$, respectively. This explanation will be further supported by analyzing the fast time-resolved experiments (*vide infra).* A further more moderate effect that should be mentioned is the fact that the association constant of BXV^{4+} per branch slightly decreases upon increasing the number of dialkoxybenzene chains to the photosensitizer. This is observed for the one-shell and two-shell photosensitizers. The lowering in the association constant per branch of BXV^{4+}, upon increasing the number of branches, is attributed to enhanced steric and/or electrostatic hindrance for binding successive units of BXV^{4+} in the multireceptor photosensitizers possessing a larger number of branches.

Static Quenching Analysis. Our discussion attributed the decrease in the observed initial luminescence intensities of the transients of **2**−**5** upon addition of BXV^{4+} to a fast intramolecular electron transfer quenching of the excited photosensitizer in the supramolecular assemblies, S^*A_n, eq 6. This fast decay of the luminescence due to static quenching of the excited photosensitizer within the supramolecular assemblies could be time-resolved using a short-pulse laser. Figure 8 shows the decay of the emission intensity of photosensitizers **2**−**5**, in the absence and in the presence of different concentrations of BXV^{4+}, within a time scale of a few nanoseconds. We clearly observe, especially for **2** and **4**, that upon addition of BXV^{4+} a fraction of the luminescence decays within a few nanoseconds until a nearly constant emission intensity is reached. The relative contribution of the fast decay corresponds to what we referred to at longer time scale emission measurements (Figure 2) as the "decrease in the observed initial emission intensity". We can therefore attribute the fast decay observed on a short time scale (Figure 8) to the static quenching of the excited photosensitizer within the supramolecular assemblies, whereas the remaining nearly constant emission is assigned to the slow decay of the luminescence of the free photosensitizer by the natural decay and diffusional quenching, which can only be observed on a longer time scale, as in Figure 2.

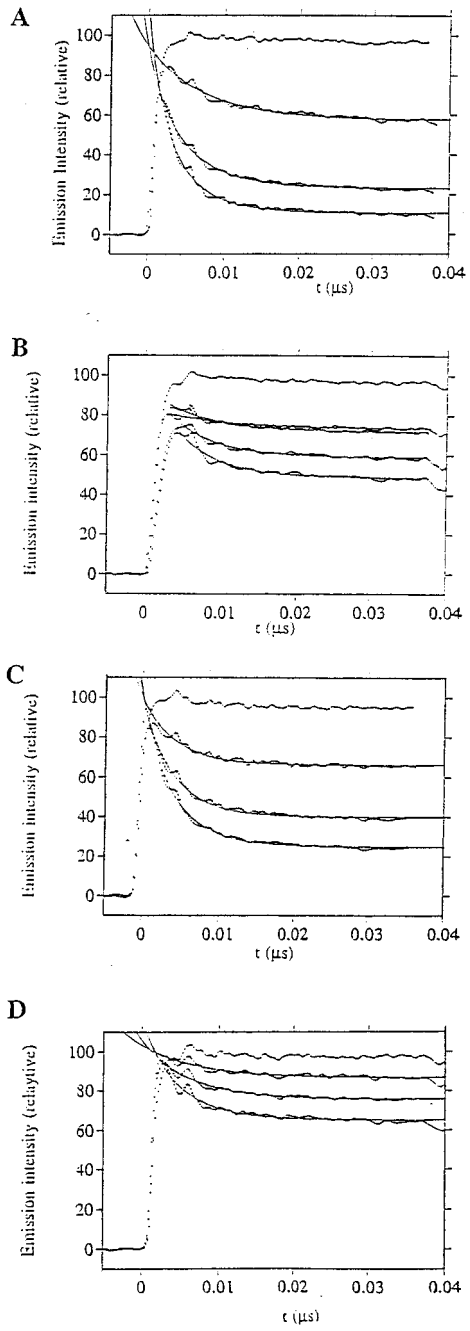

Figure 8. Decay of the emission intensity of photosensitizers (A) **2**, (B) **3**, (C) **4**, and (D) **5**, within a time scale of a few nanoseconds, in the presence and absence (upper curves) of BXV^{4+}. The transients correspond, from top to bottom in each frame, to BXV^{4+} concentrations: 0, 1.7×10^{-3}, 3.3×10^{-3}, and 5.0×10^{-3} M. Least-squares fitting curves are overlaid on the experimental points.

The fast transients shown in Figure 8 exhibit two important features. First, the contribution of the fast decay increases with increasing concentration of BXV^{4+}, and no fast decay is observed in the absence of BXV^{4+}. The relative contribution of the fast decay is equal to the fraction of photosensitizer bound to one or more BXV^{4+} units, which is calculated from eq 10 and the values of K displayed in Table 1. For this reason, the fast decays observed for **3** and **5**, which are poorly binding to BXV^{4+}, have a smaller contribution than the fast decays observed for **2** and **4** with the addition of similar concentrations of BXV^{4+}. Second, the fast decay becomes faster with increasing concentration of BXV^{4+}. That is, if one tries to fit these fast decays to a monoexponential decay, one finds that the decay constant becomes larger with increasing BXV^{4+}

(22) (a) Allwood, B. L.; Spencer, N.; Shahriari-Zavareh, H.; Stoddart, J. F.; Williams, D. J. *J. Chem. Soc., Chem. Commun.* **1987**, 1064. (b) Ashton, P. R.; Chrystal, E. J. T.; Mathias, J. P.; Parry, K. P. Slawin, A. M. Z.; Spencer, N.; Stoddart, J. F.; Williams, D. J. *Tetrahedron Lett.* **1987**, *28*, 6367. (c) Odell, B.; Reddington, M. V.; Slawin, A. M. Z.; Spencer, N.; Stoddart, F. J.; Williams, D. J. *Angew. Chem., Int. Ed. Engl.* **1988**, *27*, 1547.

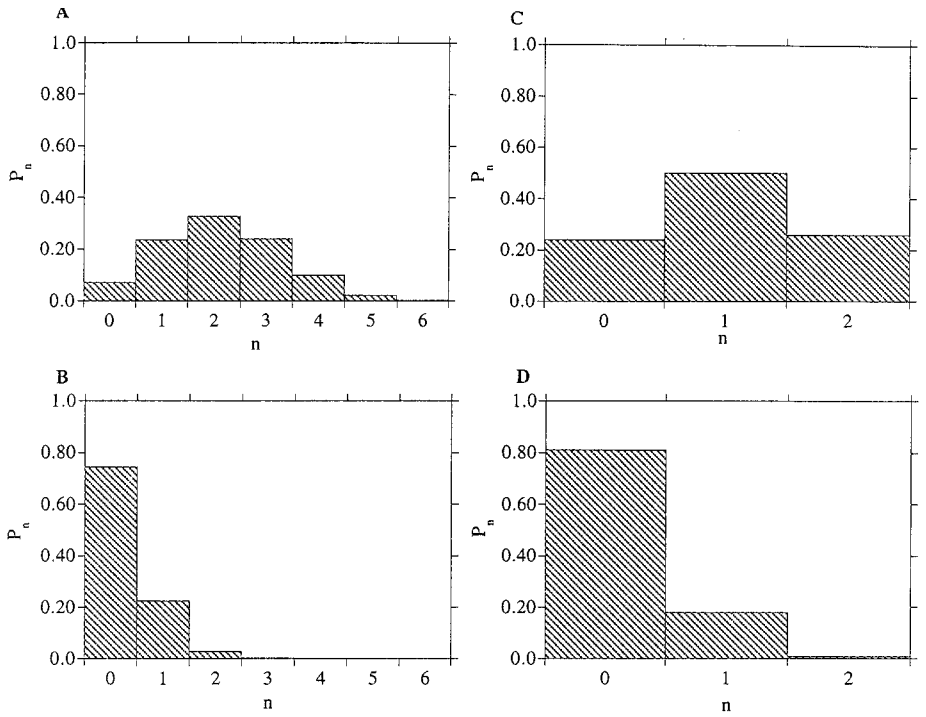

Figure 9. Histograms representing the equilibrium statistical distribution of stoichiometries of the supramolecular assemblies formed by (A) **2**, (B) **3**, (C) **4**, and (D) **5**, in the presence of BXV^{4+} (5.0×10^{-3} M), according to eq 10 and calculated values of *K*.

concentration. The acceleration of the fast luminescence decay with increasing concentration of BXV^{4+} is attributed to the fact that at higher BXV^{4+} concentrations more significant populations of higher supramolecular stoichiometries are found in the systems. The presence of a larger number of electron acceptor units within the supramolecular assemblies enhances the probability of electron transfer, as assumed by our kinetic model. The fast transients shown in Figure 8 were properly fitted to eq 11 by means of an iterative least-squares fitting program. The term $\exp(-k_D + k_{dq}[A])t$ in eq 11 was omitted since on this short time scale it nearly equals unity, and only the parameters $I(0)$, $K[A]$, and k_{sq} were optimized. The fitted curves are overlaid on the experimental transients shown in Figure 8. For each photosensitizer, all the fitted curves corresponding to different concentrations of BXV^{4+} yielded nearly the same values of $I(0)$, and similar values of k_{sq}. The results are summarized in Table 1. The optimized values for $K[A]$ varied with the concentration of BXV^{4+}, and the derived *K* values from the different transients are almost identical (presented in Table 1 in parentheses). The values of the association constants of BXV^{4+} to the photosensitizers are comparable to the values obtained from the modified Stern−Volmer plots.

One important point to note about the results of the fast time-resolved emission measurements is that the rate constants of the static quenching, k_{sq}, obtained for all the photosensitizers are on the same order of magnitude. If the electron acceptor BXV^{4+} units would associate in the two-shell photosensitizers **2** and **4**, to the peripheral dialkoxybenzene groups rather than to inner shell dialkoxybenzene groups, then k_{sq} for **2** and **4** would be expected to be substantially lower than the k_{sq} values for **3** and **5** due to the exponential distance dependence of the electron transfer rate. For example, in our studies on photoinduced electron transfer in supramolecular assemblies composed of alkoxyanisyl-tethered Ru(II)−tris(bipyridazine) complexes and BXV^{4+}, elongation of the triethylene glycol bridges by one additional ethylene glycol unit led to a 5-fold decrease in the static quenching rate constant. In the present case, however, addition of a triethylene glycol chain spacing the dialkoxybenzene sites does not decrease the static quenching rate constant by more than 25%. That is, in both the one-shell and two-shell multireceptor photosensitizers, the bound BXV^{4+} units are found at nearly the same distance from the Ru(II)−tris(bipyridine) chromophore. This fact implies that the BXV^{4+} units are found near the inner-shell dialkoxybenzene group and supports our previous conclusion that both inner and peripheral dialkoxybenzene groups of each branch participate in the association of one BXV^{4+} unit.

The superior electron transfer quenching reactions in the two-shell multireceptor photosensitizers **2** and **4**, compared with the analogous one-shell multireceptor photosensitizers **3** and **5**, respectively, can be quantitatively explained by showing the statistics of the different supramolecular stoichiometries coexisting in solutions consisting of the same concentrations of photosensitizer and electron acceptor. The histograms shown in Figure 9 represent the distribution of supramolecular photosensitizer−acceptor complexes of variable stoichiometries, calculated from eq 10 and the derived values of *K*, corresponding to solutions containing **2**−**5** (4.5×10^{-5} M) and BXV^{4+} (5.0×10^{-3} M). For the two-shell multireceptor photosensitizer **2**, Figure 9A, which includes six branches, only 7% of the photosensitizer is unbound. The highest population of supramolecular assembly corresponds to one photosensitizer which is associated to two BXV^{4+} units ($n = 2$), slightly lower populations of $n = 1$ and $n = 3$ stoichiometries complete most of the supramolecular structures, and significant populations of $n = 4$ and $n = 5$ coexist in the system. The analogous one-shell photosensitizer **3**, is, however, mostly unbound (ca. 75%), with about 20% bound to one BXV^{4+} unit and a very low portion of a supramolecular $n = 2$ stoichiometry. A larger population of higher stoichiometries leads to (i) a higher contribution of the static quenching mechanism to the overall decay of the excited states and (ii) a faster static quenching, since the rate of static quenching is proportional to the number of electron acceptor units bound to the photosensitizer. A similar effect can be observed for the two-branched multireceptor photosensitizers **4** and **5**, as shown by histograms B and D in Figure 9. In the two-shell photosensitizer **4**, only ca. 25% of the chromophore exists in a free state whereas the rest of the

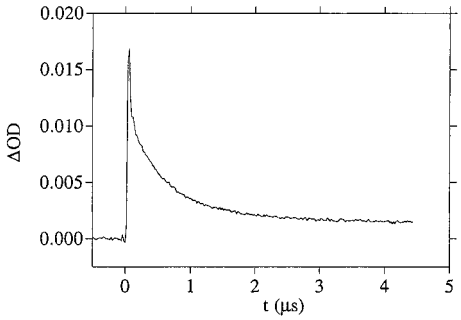

Figure 10. Transient decay of the reduced photoproduct $BXV^{\bullet 3+}$ formed upon excitation of **2** in the presence of BXV^{4+} (2.5×10^{-3} M) as a result of back electron transfer. Reduced photoproduct was followed at $\lambda = 600$ nm.

photosensitizer is present as a supramolecular structure of stoichiometries $n = 1$ (ca. 50%) and $n = 2$ (ca. 25%). In the one-shell photosensitizer, ca. 80% of the chromophore is present in the free state and the rest is bound to only one BXV^{4+} unit.

This analysis accounts in detail for the effectiveness of intramolecular electron transfer quenching in the one-shell and two-shell photosensitizers that include tethered dialkoxybenzene receptor sites for BXV^{4+}. Increasing the number of dialkoxybenzene chains on the central Ru(II)−bipyridine photosensitizer enhances the static electron transfer quenching in either one-shell or two-shell photosensitizers. This is due to the enriched population of supramolecular complexes with BXV^{4+}, and particularly complexes exhibiting higher stoichiometries, upon increasing the number of branches tethered to the photosensitizer. The most important effect that controls the intramolecular electron transfer quenching is, however, noticed upon comparison of the one-shell and two-shell dialkoxybenzene-functionalized photosensitizers. The static quenching is favored in the two-shell photosensitizers, where high populations of the supramolecular assemblies with BXV^{4+} are present. The high populations of the supramolecular assemblies in the presence of the two-shell photosensitizers originate from the high binding affinities of BXV^{4+} to these photosensitizers. The improved binding constants of BXV^{4+} to the two-shell photosensitizers are attributed to a cooperative binding of the two dialkoxybenzene units to BXV^{4+}, forming π-stacked supramolecular systems. In this context, it is illuminating to compare the effectiveness of intramolecular electron transfer quenching in the two-branched two-shell photosensitizer **4**, to that of the six-branched one-shell photosensitizer **3**, parts C and B of Figure 2, respectively. Although **3** includes six dialkoxybenzene binding sites, the intramolecular quenching in **4** that includes only four dialkoxybenzene units is significantly more efficient. The derived histograms of the supramolecular assemblies in the presence of **3** and **4**, Figure 9B,C, clearly reveal that, for the two-shell photosensitizer **4**, only ca. 20% of the chromophore exists in the free state, whereas for the one-shell photosensitizer **3**, ca. 75% of the chromophore is in the free configuration.

Back Electron Transfer Analysis. Finally, we examined the electron transfer products formed upon quenching of the excited states both via the static mechanism, within the supramolecular assemblies, and via the diffusional pathway. Figure 10 shows the transient decay of the absorbance of $BXV^{\bullet 3+}$ at $\lambda = 600$ nm, formed upon excitation of **2**. It exhibits an absorbance at $\lambda = 600$ nm, characteristic of the radical cation of bipyridinium salts. Since no oxygen and no secondary electron acceptor is present, we attribute the decay of the absorbance at 600 nm to the recombination of the redox products, i.e., to the back electron transfer from $BXV^{\bullet 3+}$ to the oxidized chromophore Ru(III)−tris(bipyridine). This absorption

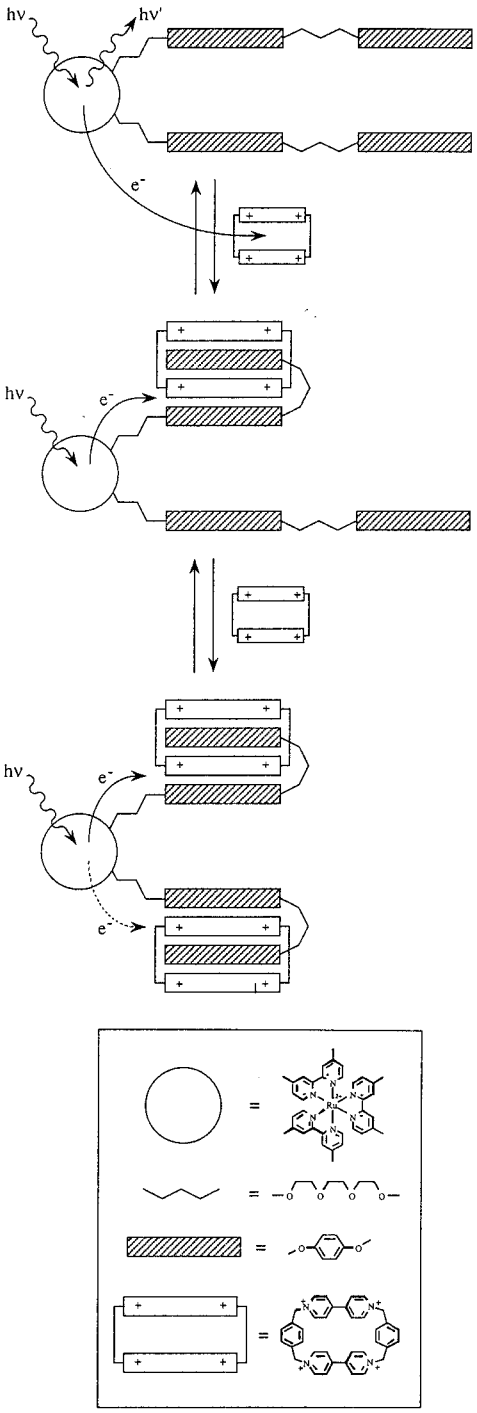

Figure 11. Schematic representation of the different molecular and supramolecular species coexisting in a system containing photosensitizer **4** and BXV^{4+}, and the different photoinduced processes they undergo upon irradiation.

decay includes a relatively fast exponential decay and a slow component which decays on a much longer time scale. The fast first-order decay is attributed to back electron transfer from the bound reduced acceptor $BXV^{\bullet 3+}$, to the oxidized chromophore, within the supramolecular assemblies (eq 8). The slow decay is attributed to the diffusional back electron transfer between the reduced acceptor and an oxidized photosensitizer which are not associated (eq 7). The static back electron transfer recombination rate constant of the photoproducts is obtained by first-order analysis of the fast component of the absorption decay shown in Figure 10, $k_{sr} = 1.6 \times 10^6$ s^{-1}. The slow component of the recombination, decaying on a long time scale of ca. 1 ms, could not be accurately analyzed, and the second-

order diffusional recombination rate constant is estimated to be $k_{dr} \approx 4 \times 10^5$ M^{-1} s^{-1}.

The efficiency of the diffusional recombination with regard to the overall recombination of the photoredox products corresponding to the relative contribution of the slow absorption decay in Figure 10 is calculated to be $\theta_{dr} = 0.14$. It is interesting to compare this efficiency of diffusional recombination with the efficiency of diffusional quenching. The latter corresponds to the fraction of unbound photosensitizer multiplied by the fraction of the unbound photosensitizer which is quenched by the diffusional mechanism, that is $\theta_{dq} = ([S]/S_o)k_{dq}[A]/(k_D + k_{dq}[A])$. From eq 10 and the values listed in Table 1, we calculate a value of $\theta_{dq} = 0.13$, which is similar to the efficiency of diffusional recombination. From this comparison we conclude that the population of redox products formed upon static quenching recombine by a static back electron transfer pathway, and the redox products formed by the diffusional quenching route recombine by a diffusional recombination pathway. Thus, there is no significant escape of redox products from the supramolecular assemblies, $k_{esc} \ll k_{sr}$ (eqs 8 and 9). The results exemplified for the photoinduced electron transfer and back electron transfer between **2** and BXV^{4+} are essentially similar for the other photosensitizers.

The inefficiency of the escape of the $BXV^{\bullet 3+}$ from the supramolecular assemblies can be attributed to the fact that although one of the bipyridinium moieties of BXV^{4+} loses its π-acceptor character upon reduction, the other bipyridinium moiety is still capable of binding to the dialkoxybenzene units tethered to the Ru(II)−bipyridine complexes **2**−**5**. Thus, the supramolecular assemblies formed by noncovalent association of BXV^{4+} to the functionalized multireceptor photosensitizers behave as intact dyads (or polyads) where the electron transfer quenching and back electron transfer proceed in the same complex, even though the supramolecular assemblies exhibit labile exchangeable structures (on longer time scales).

Figure 11 shows schematically the coexisting supramolecular assemblies formed by the two-shell photosensitizer **4** and the electron acceptor BXV^{4+}. The drawing represents the double-branch photosensitizer with two dialkoxybenzene groups in each branch, where the upper species represents the free photosensitizer, the middle species is the supramolecular assembly formed with one BXV^{4+} unit, and the bottom component is the photosensitizer−acceptor supramolecular complex with stoichiometry $n = 2$. The three species are found in equilibrium prior to irradiation. Upon photoexcitation ($h\nu$), the free photosensitizer (top) undergoes radiative emission ($h\nu'$), and is simultaneously quenched via a diffusional route. The two supramolecular assemblies undergo static electron transfer. The supramolecular assembly with higher stoichiometry (bottom) undergoes faster electron transfer due to the existence of alternative directions of charge transfer (represented by the dotted arrow). We have shown that photoinduced electron transfer occurs in the supramolecular assemblies and that the electron transfer products are stable in the resulting structure and do not dissociate within their lifetime.

The formation of the intermolecular complexes between the Ru(II)−bipyridinium photosensitizers and BXV^{4+} represents a novel means to generate noncovalently-linked photosensitizer−acceptor dyads. It should be noted that the lifetime of the redox photoproducts Ru^{3+}− $BXV^{\bullet 3+}$ in the various systems is relatively long, 0.6−0.8 μs. This value is substantially longer than the lifetime observed in covalently-linked Ru(II)−tris(bipyridine)−bipyridinium dyads[10] (ca. 20 ns). In the present systems, the dialkoxybenzene groups, acting as the active binding sites for assembling the Ru(II)−tris(bipyridine)−bipyridinium complexes, are tethered to the chromophore by relatively long and flexible polyethylene glycol bridging chains. Association of BXV^{4+} to the binding sites results in electrostatic repulsive interactions between the Ru(II) center and the acceptor component. These repulsive interactions can induce the stretching of the bridging chain with a concomitant spatial separation between the redox products. The distance imposed by the electrostatic repulsion stabilizes the photoproducts against back electron transfer.

Conclusions

The present study has demonstrated novel means to organize supramolecular photosensitizer−electron acceptor dyads and polyads by tailoring one-shell and two-shell photosensitizers that include tethered π-donor dialkoxybenzene groups. Formation of supramolecular assemblies between the photosensitizers and BXV^{4+} via π-donor−acceptor interactions leads to noncovalently-linked dyads and polyads exhibiting effective internal electron transfer. A major contribution of the present study includes the tailoring of two-shell dialkoxybenzene-functionalized photosensitizers that reveal improved affinities to form the supramolecular assemblies with BXV^{4+} due to cooperative association of the electron acceptor by the two π-donor sites. Effective internal electron transfer quenching proceeds within the resulting supramolecular assemblies, via a static quenching mechanism. Mechanistic analysis of the intrasupramolecular electron transfer quenching and the back electron transfer of the photogenerated redox products within the supramolecular systems revealed several important features.

(i) The electron transfer quenching proceeds in two distinct populations of the photosensitizer that include supramolecular assemblies of the photosensitizer−acceptor components and free photosensitizer that is quenched via a diffusional pathway.

(ii) For multireceptor photosensitizers, which contain several binding sites for the electron acceptor, supramolecular assemblies of variable stoichiometries SA_n up to complete occupation of all binding sites are formed. For example, for the hexadentate photosensitizer **3**, formation of complexes of stoichiometries SA, SA_2, ..., SA_6 is supported by mechanistic analysis of the electron transfer quenching. Functionalization of the supramolecular photosensitizer−acceptor assembly by a high number of electron acceptor units enhances the static electron transfer quenching.

(iii) Similar analyses reveal that in the multireceptor photosensitizers containing two binding sites on each chain, namely **2** and **4**, both binding sites participate cooperatively in the association of one electron acceptor unit. Thus, each chain functions as a bidentate ligand for one acceptor unit, and then the stoichiometry of the supramolecular assemblies is determined by the number of chains rather than by the number of binding sites. For example, the dodecadentate photosensitizer **2** forms with BXV^{4+} complexes of stoichiometries SA, SA_2, ..., SA_6, similar to photosensitizer **3**. The two-shell multireceptor photosensitizers reveal stronger association to BXV^{4+} than the analogous one-shell multireceptor photosensitizers, due to an increase in the noncovalent bonding order, which stabilizes the supramolecular assemblies.

(iv) The electron transfer products formed in the systems reveal two distinct populations consisting of the redox product formed within the supramolecular assemblies and redox products formed via diffusional quenching of free photosensitizers. The two populations of redox products are nonexchangeable within the lifetime of back electron transfer.

(v) The lifetime of the redox products in the resulting supramolecular assemblies is relatively long as compared to

covalently linked dyad systems. This is attributed to the fact that the binding sites are tethered to the chromophore by long-chain spacing bridges. Electrostatic repulsion between the electron acceptor units and the photosensitizer center results in stretched conformations of the dyads, and the resulting spatial separation of the redox products stabilizes them against back electron transfer.

We conclude that although the series of photosensitizers **2**−**5** and the electron acceptor BXV^{4+} (**1**) consist of dynamic systems, the electron transfer quenching and the recombination of the photogenerated redox products proceed in static supramolecular photosensitizer−acceptor assemblies. The present systems represent the further development of supramolecular model systems for the photosynthetic reaction center. We believe that tailoring the photosensitizer with additional functional groups, e.g., linkage of an electron acceptor between the two dialkoxybenzene sites, could lead to novel and effective photosynthetic model systems and optoelectronic devices.

Acknowledgment. This research is supported by the Volkswagen Stiftung, Germany and by the James Frank Minerva Foundation (I.W.).

JA9703382